

SIMPLE AND ACCURATE AC CALORIMETER FOR LIQUID CRYSTALS AND SOLID SAMPLES

M. Castro and J. A. Puértolas

Dpto. de Ciencia de Materiales, Centro Politécnico Superior, I. C. M. A. Universidad de Zaragoza, C. S. I. C., 50015 Zaragoza, Spain

Abstract

We have designed, built and calibrated a microcomputer-controller automated a.c. calorimeter for liquid crystals and solid samples, in the temperature range from 30 to 250 °C, in which we enhance several features of previous ones reported in the literature. We have incorporated the lock-in amplifier model 5302 from EG&G in our set-up, which permits to extend the frequency range to 1 mHz. This allows the performance of suitable frequency sweeps in order to choose the optimum operating frequency for low thermal conductivity materials. The calorimeter has been calibrated with the 8OCB liquid crystal compound. The resolution obtained for C_p values was better than 0.1% and the absolute error around 5%. As applications, we show the ferroelectric transition of the triglycerine sulphate (TGS), the Nematic-Smectic A transition of the 8OCB and a study in a binary system of ferroelectric liquid crystals, SCE9-SCE10.

Keywords: AC calorimetry, ferroelectricity, liquid crystal, phase transition

Introduction

The AC calorimetry enables the thermal characterization of small mass samples (less than 100 mg) where the traditional adiabatic calorimetry does not have enough resolution. In spite of its poor absolute accuracy (5–10%), its high relative accuracy (typically 0.1%) permits to analyse transitions with small entropy content, imperceptible with other thermal methods, and to study critical behaviour since reduced temperatures of about 10^{-4} are typically reached. This technique has showed amply its applications with solid and liquid samples, and samples with high or low thermal conductivity [1].

In the last years, the appearance of new lock-in detectors in the market, with lower frequency range, has allowed to apply the same synchronous detection technique used in metal, alloys and in general for high thermal conductivity systems, to the low thermal conductivity materials as liquid crystal and organic materials [2, 3], in which we have to use an operating frequency range from 10 mHz to 1 Hz. On the other hand, the high sensitivity of this set up also permits to measure the heat capacity in solid samples without a mechanically chopper

light, as source of modulated input power. Since the phase shift resolution is 0.001 degrees, it permits to carry out phase transition character studies, because the phase presents strong variation when passing through first order transitions.

We describe an AC calorimeter for liquid crystals and solid samples in the range from 30 to 250°C, enhancing some features of other calorimeters reported in the literature [2, 3]. As applications we show some critical behaviour on solid sample, as the ferroelectric transition of TGS, and the Nematic-Smectic A transition on the liquid crystal 8OCB. In addition we present the studies of the Smectic A - chiral Smectic C (C*) line transition of the binary ferroelectric liquid system SCE9-SCE10, in order to know if this line presents a tricritical point close to the NAC point and which are the features involved in that behaviour.

Method

The basis of this method is the modulation of the heat supplied to the sample and the measurement of the temperature oscillation produced in the sample around its average value. Following as a model a slab-shaped sample, heating one of its faces with a periodic power ($P = P_o \cos 2(\omega t / 2)$) assuming one-dimensional flow and a thermal link K_b between sample and bath, the sample temperature can be written [4]: $T_s = T_b + T_{dc} + T_{ac} \cos(\omega t + \Phi)$ where

$$T_{ac} = \frac{P_o}{2\omega C_s} \left[1 + \frac{1}{\omega^2 \tau_1^2} + \omega^2 \tau_2^2 + A \right]^{-\frac{1}{2}} \quad T_{dc} = \frac{P_o}{K_b}$$

T_{dc} is the average value of the temperature difference between the bath and sample, T_b the bath temperature and T_{ac} the oscillation amplitude. τ_1 is the relaxation time from the sample to the surrounding and τ_2 is the internal thermal relaxation time of the sample. The A term is almost temperature independent and negligible. For an appropriate choice of the heating frequency such that $\omega \tau_2 \ll 1 \ll \omega \tau_1$ the amplitude is inversely proportional to the sample heat capacity, C_s .

Calorimeter

A schematic diagram of the experimental system is shown in Fig. 1. The calorimeter has two concentric cylindrical copper blocks surrounding the sample, both with external gold-plated. It can be dismantled easily since the different parts are linked by screws tightened down over high temperature O-rings without almost any soldered joints. The electrical leads with teflon insulation reach

the copper blocks through thin stainless tubes and they are thermally anchored to both blocks.

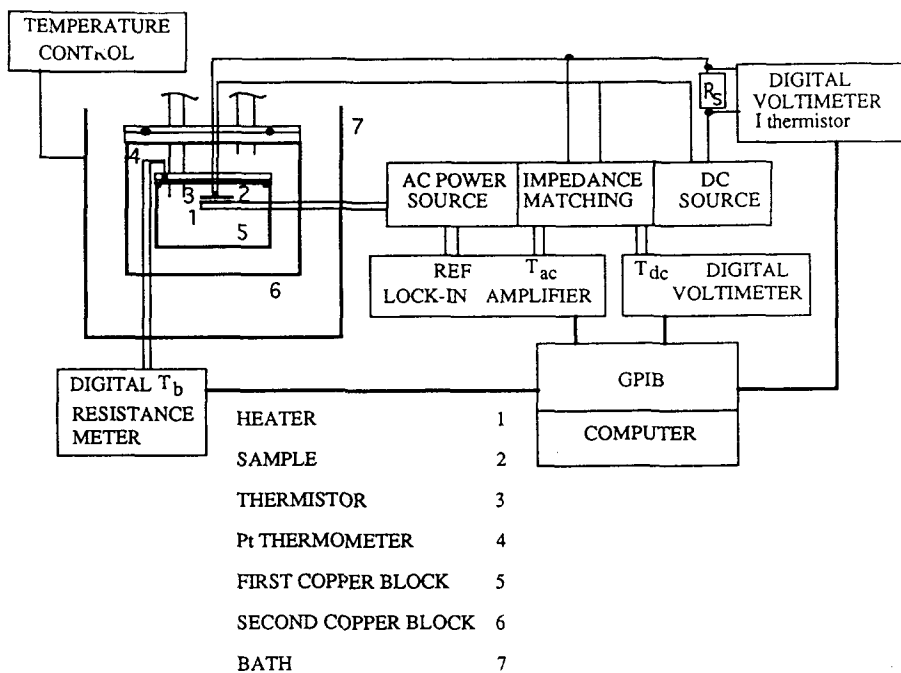


Fig. 1 Schematic diagram of the experimental system

The calorimeter is submerged in a Lauda model KP-20 temperature bath with different fluids depending of the temperature range. It is available to perform vacuum or introduce helium gas, independently in the external block or in the sample chamber, reducing or increasing the thermal contact between sample and surroundings. The external block as a thermal shield, with 10^{-1} mbar pressure of helium gas in the cavity between the two copper blocks, damps the thermal fluctuation coming from the bath (close to ± 5 mK) down to less than ± 1 mK in the temperature sample when the bath is controlling at constant temperature. The commercial bath allows to perform continuous temperature sweep and typical selected scan rate ranges between 0.1 and 1 mK/h. The average temperature of the sample has a deviation from the linearity lower that 0.01 % of the typical ramp.

Around the internal block, a heater is wound in order to perform temperature step measurements by means of an additional external controller which temperature sensor is a miniature bead thermistor (RS components International). Absolute temperatures and measurement of T_b are provided by a MINCO Platinum thermometer model S1059 calibrated at fixed points defined

by ITS-90. It is placed in a hole in the top of the internal block. Silicone is used in order to increase the thermal contact. The sample is placed inside the internal block. Liquid crystals fill a commercial DSC cell (10 μl) or a cell constructed with thin silver foils chemically inert with respect to the sample. The use of DSC capsule permits to make direct comparison with DSC experiment in the same sample.

The ac heat input is supplied by a strain gauge, from OMEGA Inc. with a nominal resistance of 120 Ω , fixed to the sample or liquid crystal cell using GE varnish 7031. The strain gauge is at the same time the sample support. In order to measure the temperature oscillation and the average sample temperature we attach to the opposite face of the sample, a microbead thermistor from Victory Engineering Corp. ($R=106 \Omega$ at 25°C) with GE varnish. The constant dc current coming from stable battery applies to the thermistor ranges between 0.5 and 10 μA depending on the temperature range and it has a fluctuation lower than 0.01%. Thermistor constants are obtained by calibrating the thermistor resistance values against the Pt thermometer during each measurement in some points at constant temperature. The rms heater power ranges from 0.4 to 6 mW reaching ac amplitudes from 50 to 300 mK and typical T_{dc} value from 0.3 to 1 K.

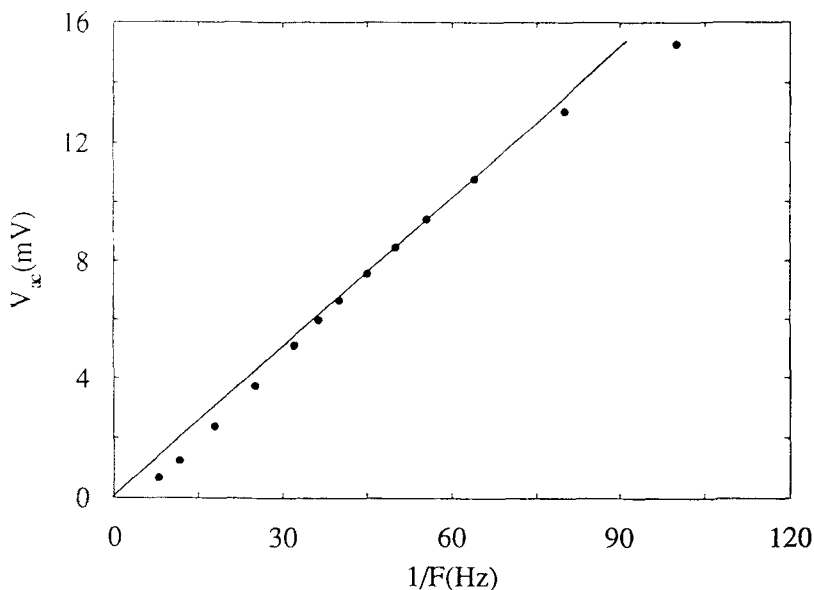


Fig. 2 Frequency response at room temperature of the 8OCB sample

We incorporate the lock-in model 5302 from EG&G in the set-up, with an operating frequency range down to 1 mHz. The lock-in oscillator drives the

sinusoidal voltage applied to the strain gauge, and it measures the ac amplitude, V_{ac} , and the phase of the thermistor voltage when is locked in the $2F$ mode, because the frequency of the ac temperature is twice that of the heating voltage. Besides, we can obtain by measuring $V_{ac}(\omega)$, the optimum frequency in order to verify $\omega\tau_2 \ll 1 \ll \omega\tau_1$. As an example, the Fig. 2 plots the frequency response of the 80CB sample, V_{ac} vs. $1/\omega$, in which we realize the linear region centered about 20 mHz, which is chosen as the working frequency. The average value of the sample temperature is determined from a sampling of the thermistor voltage in some periods with the HP 3457A digital voltameter. The current supplied to the thermistor is measured with a Fluke 8840A digital voltameter in order to obtain the thermistor resistance. All the data acquisition is controlled by a PC computer by means of a program written in Basic language.

This measuring system allows to extend the technique in order to measure C_p in the frequency domain (Heat Capacity Spectroscopy), for this application is necessary to use the $3F$ mode from the lock-in amplifier. This spectroscopy is applied to study relaxation processes near the glass transition on polymers and supercooled liquid [5].

Application

Solid samples

As solid sample, we have measured the ferroelectric transition of a TGS crystal (16.3 mg) from 30 to 70 °C. The Fig. 3 shows the step in the heat capacity predicted by the mean field theory after subtract an extrapolated baseline. The maximum dispersion is lower than $\pm 0.2\%$ of the total C_p measured. If we introduce the fluctuation contribution to uniaxial ferroelectric material, the heat capacity at $T > T_c$ but near the transition, it must show a logarithmic dependence with the temperature. This behaviour is showed in the upper inset in Fig. 3 similar to the reported in the literature [6].

Liquid crystals

The Fig. 4 shows the sequence of phase transitions of the 80CB thermotropic liquid crystal. In the Nematic (N)-Smectic A (A) transition we find a sharp and symmetrical peak. These data, after subtracting a linear baseline calculated from the data out the transition, have been plotted vs. the reduced temperature (Fig. 4). In order to estimate the critical exponent, power-law fits have been made. The obtained exponents are in the range 0.23–0.38, giving similar good results and showing clearly that the data are not consistent with a 3d XY behaviour where it is expected a nearly logarithmic singularity. Our results are in agreement with the literature [3, 7].

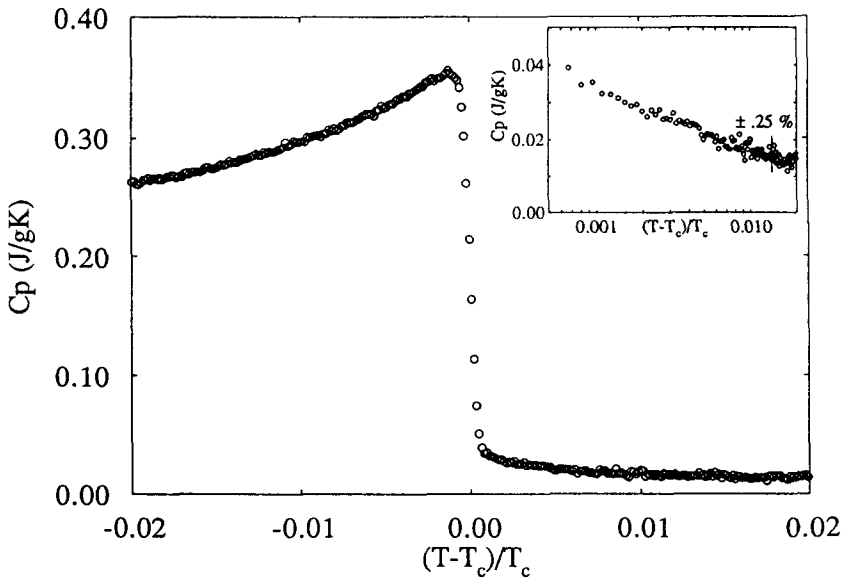


Fig. 3 Heat capacity near the transition of triglycine sulphate (TGS). The inset show the logarithmic dependence of the heat capacity tail

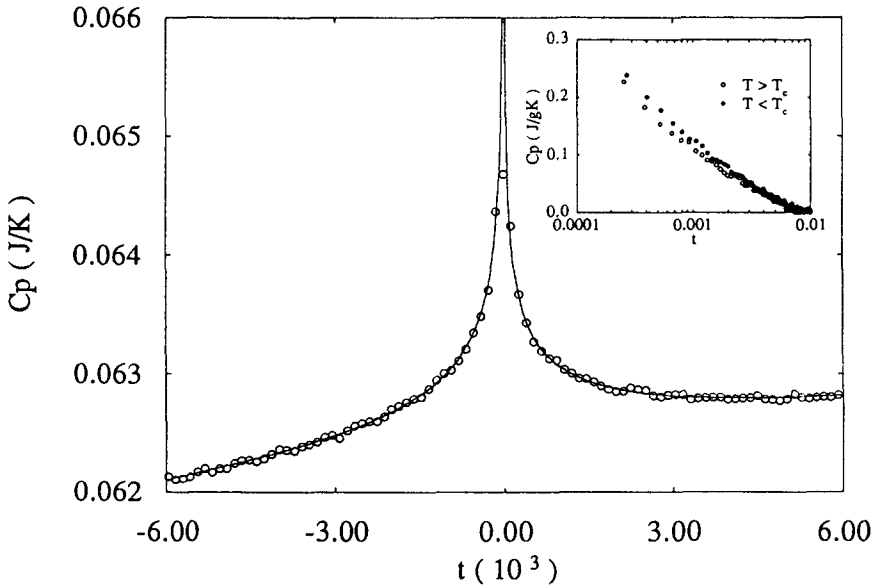


Fig. 4 Heat capacity of the 8OCB sample near the nematic-to-smectic A transition. Inset: semilogarithmic plot of the heat capacity after subtracting an extrapolated baseline

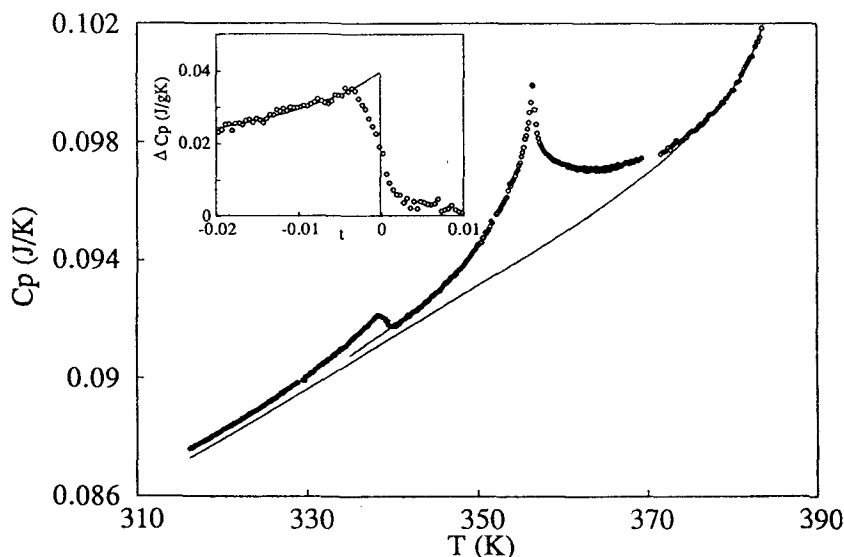


Fig. 5 Experimental heat capacity for the SCE9-SCE10 mixture ($x=0.48$) with the baselines used to obtain the ΔC_p associated to the A-C* (inset) and N-A transition. The continuous curve in the insert represent the fit to the extended Landau model

Phase diagram of commercial binary mixture of two compounds SC9 and SC10 with respectively phase sequences Isotropic (I)-Chiral Nematic (N)-Chiral Smectic C(C*) and I-N-A-C* have been investigated by spontaneous polarization and ac calorimetry [8]. The figure shows the A-C* and N-A transitions in one of the mixture ($x=0.48$, 48 wt. % of SCE9). We focus the study on the second order transition A-C line in order to know the existence or not of a tricritical point close to NAC point. The insert of Fig. 5 shows the analysis of excess heat capacity ΔC_p due to the A-C* transition using the so-called extended Landau model with $\Delta C_p/T = A/T_c^2 ((T_m - T)/T_c)^{-1/2}$. The result for the studied dilutions point out that the second order regime of A-C* line toward tricritically as the NAC* point is approach and that this behaviour is controlled by the decreasing of the A range, the proximity of the I phase to the A phase, in addition to the high dielectric moment presented in these compounds.

* * *

This work was supported by the C. I. C. Y. T. Project n° MAT 91-0923-C02-02, Spain.

References

- 1 I. Hatta and A. J. Ikushima, *Jap. J. Appl. Phys.*, 20 (1981) 1995.
- 2 M. Meichle and G. W. Garland, *Phys. Rev.*, A 27 (1987) 2624.
- 3 G. W. Garland, *Thermochim. Acta*, 88 (1985) 127.
- 4 P. F. Sullivan and G. Seidel, *Phys. Rev. Rev.*, 173 (1968) 679.
- 5 N. O. Birge, *Phys. Rev.*, B. 34 (1986) 1631.
- 6 K. Ema, K. Hamano and Y. Ikeda, *J. Phys. Soc. Japan*, 46 (1979) 345.
- 7 G. Nounesis, K. I. Blum, M. J. Young, C. W. Garland and R. J. Birgeneau, *Phys. Rev. E.*, 47 (1993) 1910.
- 8 J. Zubia, M. Castro, J. A. Puértolas, J. Etxebarria, M. A. Perez Jubindo and M. R. de la Fuente, *Phys. Rev. E*, 48 (1993) 1970.

Zusammenfassung — Für Flüssigkeitskristalle und flüssige Proben wurde für den Temperaturbereich von -30 bis 250°C , in dem im Vergleich zu den in der Literatur beschriebenen einige Merkmale verbessert wurden, ein mikrocomputerkontrolliertes Wechselstrom-Kalorimeter entworfen, gebaut und kalibriert. In der Apparatur wurde das Lock-in Modell 5302 von EG&G integriert, das eine Ausweitung des Frequenzintervalles bis 1 mHz zuläßt. Dies erlaubt die Durchführung geeigneter Frequenzdurchläufe, um die optimale Betriebsfrequenz für Substanzen mit niedriger Wärmeleitfähigkeit auszuwählen. Das Kalorimeter wurde mit der Flüssigkeitskristallverbindung 80CB kalibriert. Die für C_p erhaltene Auflösung war besser als 0.1% und der absolute Fehler lag bei 5%. Als Anwendung wurde die ferroelektrische Umwandlung von Triglycerinsulfat (TGS), die nematisch-smektische Umwandlung A von 80CB sowie eine Untersuchung in einem binären System der ferroelektrischen Flüssigkeitskristalle SCE9-SCE10 gezeigt.